

The Multi Spectral Solar Telescope Array VIII: The Second Flight

A. B. C. Walker, Jr. M. J. Allen, C. E. DeForest, C. C. Kankelborg, D. S. Martinez-Galarce, J. E. Plummer,
Departments of Physics and Applied Physics and Center for Space Science and Astrophysics
Stanford University, Stanford, CA 94305-4055 USA

Richard B. Hoover
Space Science Laboratory
NASA Marshall Space Flight Center, Huntsville, AL 35812 USA

Troy W. Barbee, Jr.
Lawrence Livermore National Laboratory
Livermore, CA 94550 USA

David B. Gore
Department of Physics
University of Alabama at Birmingham, Birmingham, AL 35294

ABSTRACT

The *Multi Spectral Solar Telescope Array (MSSTA)* is a rocket borne observatory that utilizes an array of multi-layer and interference film coated telescopes to observe the solar atmosphere from the chromosphere to the corona, over a broad spectral range (VUV - soft X-rays). The *MSSTA* is continuously evolved to incorporate new instruments, and to improve its ability to investigate specific topics related to the structure and dynamics of the solar atmosphere. We describe chromospheric and coronal observations recorded during the second flight of the *MSSTA* on November, 3, 1994 at 1915 UT.

1.0 INTRODUCTION

The solar atmosphere, a strongly coupled physical system which extends over more than three decades in temperature (4,500 K to >10,000,000 K), presents a formidable observational challenge. The visible surface of the sun, the photosphere, is at ~6,000 K; above the photosphere the temperature initially decreases to ~4,500 K, and then rapidly increases to 100,000 K. This hot envelope, the chromosphere^{1,2}, is concentrated in small structures {~2,000-3,500 kilometers (3-5 arc seconds as observed from the earth) or less in size} which are arranged into a filamentary network (See figure 1a, which was obtained by the first *MSSTA* flight³, in the H Lyman α line of Hydrogen at 1216 Å). The magnetic field (figure 1b) is also concentrated in the "chromospheric network", and is ultimately responsible for the heating of the chromosphere and corona, although the precise heating mechanism, or mechanisms, are the subject of considerable debate. The magnetic fine structure at the base of the chromospheric network is composed of even smaller elements⁴, on the scale of 100 km (0.15 arc seconds as viewed from earth). Overlying the chromosphere are very hot ($T > 1,000,000$ K) plasmas (Figure 2) that are magnetically confined in the form of thin loops⁵, varying in size from a few thousand kilometers to over 100,000 kilometers. The smallest loops appear to be associated with the chromosphere network; the larger loops are associated with strong sunspot magnetic fields (Figure 1b). In order to address questions raised by the structures and dynamical behavior observed in the solar atmosphere, the *Multi-Spectral Solar Telescope Array (MSSTA)* is designed to image the atmosphere over the full range of temperatures observed, ~4,500 K to > 10,000,000 K, with sub-arc second resolution. The *MSSTA* observations address scientific questions relating to three aspects of the solar atmosphere.

- (I) *The heating and dynamics of chromospheric and coronal structures including spicules, coronal loops, bright points, and plumes; and the role of the fine scale structure of the chromospheric network in the transport of mass and energy between these structures.*
- (II) *The large scale structure of the corona, including the interface of prominences and filaments with coronal material, the transition region structure of coronal holes and plumes, and the generation of the solar wind.*
- (III) *The structure and energy balance of the coronal loops and prominences that are associated with solar flares and coronal mass ejections (CME's).*

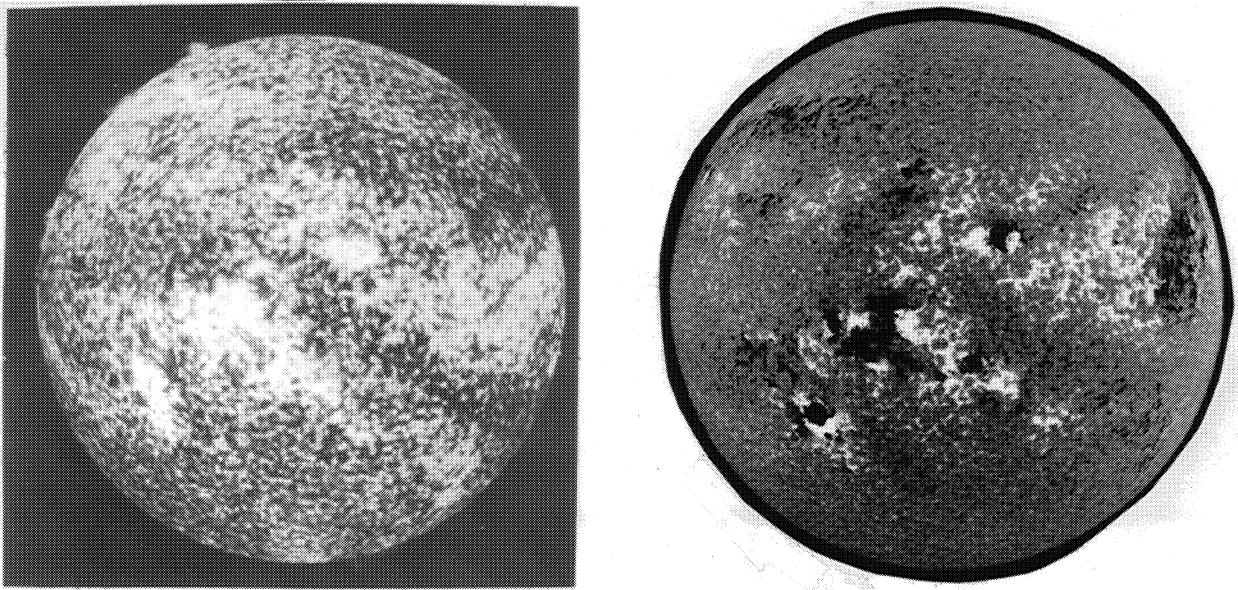


Figure 1a. (left) The chromosphere photographed in the light of H Lyman α (λ 1216 Å) by *MSSTA I* at 1905 U.T. on May 13, 1991. The resolution of the image is ~ 0.7 arc sec. The network structure and the fine vertical flux tubes called spicules are both apparent. The H Lyman α line is formed in the temperature range 25,000 K to 60,000 K. The network is composed of individual structures smaller than $\sim 5''$ in size. **Figure 1b.** (right) The solar magnetic field on May 13, 1991, as observed by the Kitt Peak Vector Magnetograph. (Courtesy of Karen Harvey).

In order to address these fundamental scientific problems, the observational objective of the *MSSTA* is to obtain sets of high resolution spectroheliograms with the following properties:

- (i) *Sufficiently broad spectral coverage to allow modeling of structures covering the full range of temperatures observed in the chromosphere and corona, $\sim 10^4$ K to 10^7 K.*
- (ii) *Sufficient spectral resolution ($\lambda/\Delta\lambda \sim 30-100$) in each spectroheliogram to allow isolation of the emission from lines excited over a narrow range of temperatures. Table 1 is a list of solar vacuum ultraviolet (VUV), far ultraviolet (FUV), and soft x-ray emission lines which are sufficiently strong to be imaged with current *MSSTA* technology.*
- (iii) *Accurate photometric calibration to permit detailed thermal modeling of the chromospheric and coronal structures observed.*

The approach we have implemented, to address the observational objectives (i), (ii) and (iii), is to obtain high resolution (~ 0.7 arc seconds) photographically recorded (in order to achieve the highest possible angular resolution) spectroheliograms in lines excited over the full range of temperatures present in the solar chromosphere, transition region and corona, by using an array of compact high resolution FUV and soft x-ray telescopes. Table 2 summarizes the characteristics of the optical systems flown in the first two *MSSTA* flights (hereafter referred to as *MSSTA I*, and *MSSTA II*), or currently under development. These instruments can obtain images in as many as 18 different wavelength intervals, thereby providing high resolution simultaneous images corresponding to as many as 18 thermal levels of the atmosphere, from Mg II ($\sim 15,000$ - $25,000$ K) and H Ly α ($\sim 20,000$ - $60,000$ K) to Fe XX ($8,000,000$ K - $10,000,000$ K).

The *MSSTA* imaging telescopes are made possible by the advances which have occurred in the fabrication of normal incidence x-ray optics using multilayer technology, and FUV/VUV optics, using interference filters. Barbee⁶ has reviewed multilayer optics technology, and Walker *et al*⁷⁻¹⁰ have reviewed the application of multilayer optics to astronomical imaging. The multilayer technology employed in the *MSSTA* is considerably more advanced than the technology employed by our consortium [Walker *et al*¹¹] in obtaining the first successful high resolution astronomical multilayer image in 1987. Zukic *et al*¹² have reviewed the fabrication and performance of reflection and transmission interference filters.

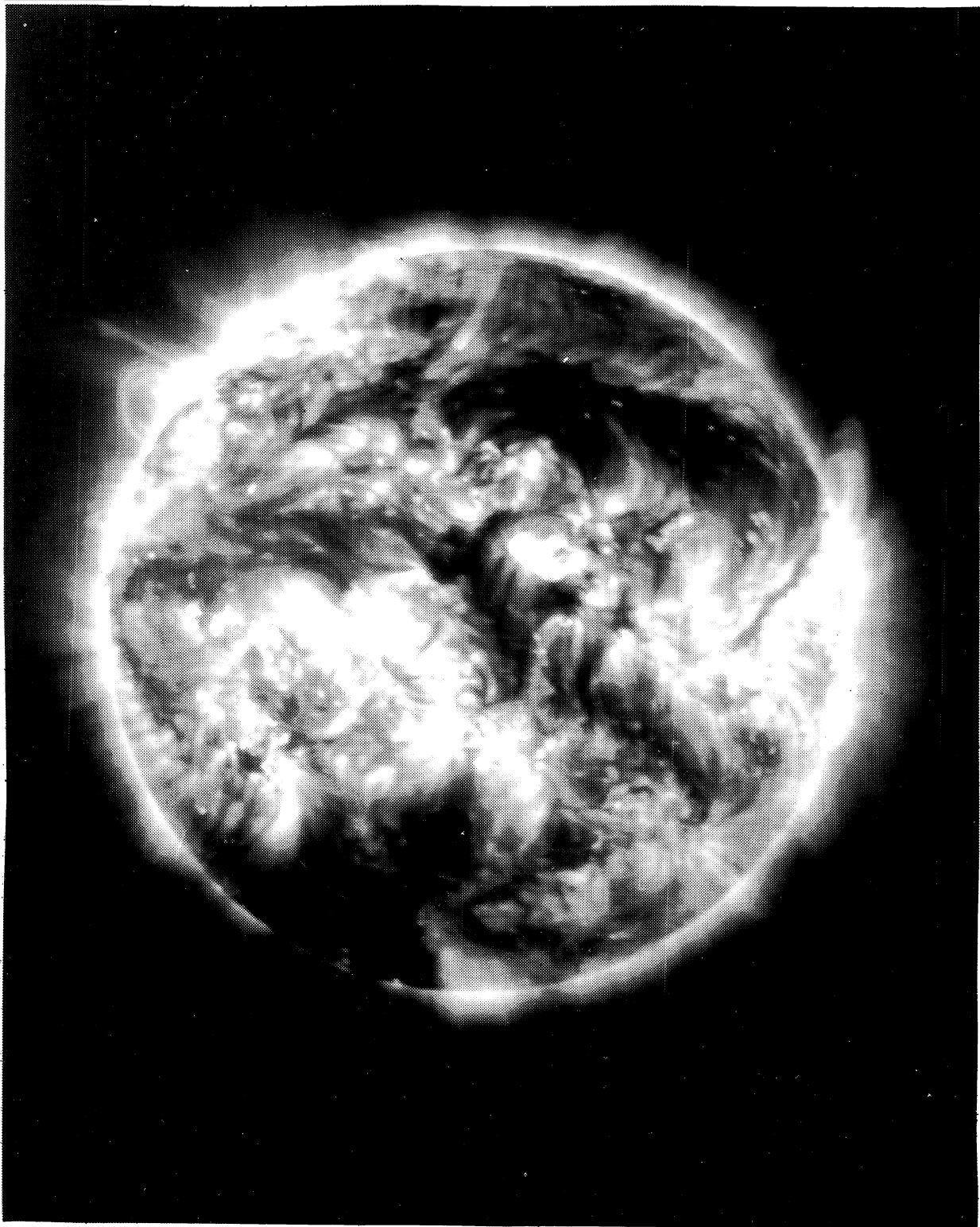


Figure 2. The corona as observed in the light of the ion Fe XII by the *MSSTA* at 1905 U.T. on May 13, 1991. The image represents the configuration of the corona at 1,500,000 K.

TABLE 1. Solar X-Ray, FUV and VUV Lines

Ion	Wavelength (Angstroms)	Temperature (Kelvins)	Solar Flux (ergs/cm ² -sec)	Ion	Wavelength (Angstroms)	Temperature (Kelvins)	Solar Flux (ergs/cm ² -sec)
He II	303.8	50,000	480 x 10 ⁻³	N I	1319.0	4,500	20 x 10 ⁻³
O VI	150.1	300,000	2.5	O I	1355.6	8,000	40
Ne V	143.3*	450,000	2.0	Fe II	1772.5	10,000	10
Ne VIII	98.1	700,000	4.2	Si II	1808.0	15,000	100
Fe IX	171.1	900,000	51.5	C II	1334.5	20,000	100
Mg X	57.9	1,000,000	4.0	Mg II	2795.4	25,000	6,000
Fe XI	180.4	1,250,000	59.0	Fe III	1914.1	25,000	50
Fe XII	195.1	1,500,000	97.0*	H I	1215.6	40,000	5,000
Si XII	44.2	2,000,000	5.0**	Si III	1892.0	50,000	150
Fe XIV	211.3	2,500,000	37.0	O III	1666.1	60,000	15
Fe XV	284.2	3,250,000	65.0	C III	1908.8	75,000	125
Fe XVI	54.7	4,000,000	9.0**	Si IV	1393.8	75,000	115
Fe XVIII	93.9	6,500,000	2.0	C IV	1548.2*	100,000	250
Fe XX	132.8	8,000,000	-.***	O IV	1401.2	125,000	15
Fe XXII	135.8	12,000,000	-.***	N V	1238.8	175,000	20
Fe XXIV	192.0	20,000,000	-.***	O V	1371.3	200,000	10

*strongest line in multiplet **total flux in multiplet * excited during flares

TABLE 2. Characteristics of The MSSTA Optical Systems

Telescope	Wave-length (Å)	Ion	Mirror Coating (Å)	Bandpass	Solar Temperature (K)	Focal Length (mm)	Aperture (mm)	f ratio	Limiting Resolution
Ritchey Chretien XII	2800	Mg II	Al/Mg ₂ F/Os	100	15,000-25,000	3500	127	27.6	0.50"
Ritchey-Chrétien XII - I	1216	H I	Al/Mg ₂ F/Os	65	20,000-60,000	3500	127	27.6	0.25"
Ritchey-Chrétien XII - V	304	He II	Mo/Mg ₂ Si	15	80,000	3500	127	27.6	0.25"
Ritchey-Chrétien XII VII	1548	C IV	Al/Mg ₂ F/Os	100	100,000	3500	127	27.6	0.33"
Ritchey-Chrétien XII - III	150	O VI	Mo/Si	7	300,000	3500	127	27.6	0.33"
Ritchey-Chrétien XII	173	Fe IX/X	Mo/Si	6	900,000	3500	127	27.6	0.33"
Ritchey-Chrétien XII - II	193	Fe XII	Mo/Si	9	1,500,000	3500	127	27.6	0.33"
		Fe XXIV (§)			20,000,000				
Ritchey-Chrétien XII - IV	284	Fe XV	Si/Mg ₂ Si	6	3,250,000	3500	127	27.6	0.33"
Herschelian XII - VI	93.9	Fe XVIII	Co/B ₄ C	1.5	6,500,000	1000	127	8.0	0.75"
Cassegrain X - 1	173	Fe IX/X	Mo/Si	6	1,000,000	2000	100	33.2	1.0"
Cassegrain X - 2	211	Fe XIV	Mo/Si	17	2,500,000	2000	63	33.2	1.0"
Cassegrain X	5000	K-corona	Al/Mg ₂ F	1000	1,500,000	750	100	7.5	3.0"
Herschelian X - A	193	Fe XII	Mo/Si	12	1,500,000	1500	100	17.5	0.5"
Herschelian X - B	211	Fe XIV	Mo/Si	14	2,500,000	1500	100	17.5	0.5"
Herschelian X - B'	54.7	Fe XVI	Co/C	0.6	4,000,000	1500	100	17.5	0.5"
Herschelian IV - δ	150	O VI	Mo/Si	9	300,000	1000	38	26.7	0.75"
Herschelian IV - θ	143	Ne V	Mo/Si	8	600,000	1000	38	26.7	0.75"
Herschelian IV - γ	180	Fe XI	Mo/Si	10	1,250,000	1000	38	26.7	0.75"
Herschelian IV - α	44	Si XII	Co/C	0.5	2,000,000	1000	38	26.7	0.75"
Herschelian IV - ζ	284	Fe XVI	Si/Mg ₂ Si	9.0	3,250,000	1000	38	26.7	0.75"
Herschelians IV - β & η	54.7	Fe XVI	Co/C	0.5	4,000,000	1000	38	26.7	0.75"
Herschelian IV - ε	93.9	Fe XVIII	Co/B ₄ C	1.5	6,500,000	1000	38	26.7	0.75"
Herschelians IV	133	Fe XX	Mo/Si	7	8,000,000	1000	38	26.7	0.75"
Herschelian IV	93.9	Fe XXI	Mo/Si	6	10,000,000	1000	38	26.7	0.75"

Notes: (§) This high temperature line is only expected to contain appreciable flux during or shortly after flares.

The *MSSTA* was flown in May, 1991^{13,14}, successfully achieving the observational goals outlined in (i), (ii) and (iii) above by obtaining high quality solar images³ of chromospheric (Figure 1a), transition region and coronal (Figure 2) structures; the best of the images achieved 0.7 arc seconds resolution. The *MSSTA* was successfully reflown on November 3, 1994. In Section 2, we discuss the reconfigured *MSSTA* instrument. In Section 3, we present some of the *MSSTA II results*, and discuss their implications for models of the solar atmosphere.

Although the *MSSTA* technology has raised the quality of coronal and chromospheric images to a new level, the limitations imposed by the constraints inherent in sounding rocket technology do not permit a number of important scientific questions to be addressed. These questions require observations with the following capabilities:

- (iv) To address I, (a) spatial resolution sufficient to resolve solar structures on a scale of 100-200 km (0.1-0.3 arc seconds); to address II, (b) images of the inner corona with resolution at least 1.0 arc second, and high sensitivity images of the extended corona (to ~ 3-4 solar radii above the limb) with resolution of ~ 3 arc seconds; for both objectives I and II, (c) direct measurements of the coronal magnetic field.
- (v) To access the role of non-thermal phenomena in the heating and dynamics of the chromosphere/corona interface, high resolution ($\lambda/\Delta\lambda > 1000$) spectroheliograms with spatial resolution of 0.3 arc seconds.
- (vi) To address III, long duration observations permitting the evolution of flares and CME's to be studied.

To achieve these levels of performance, we proposed, and NASA selected for implementation on the Space Station *Freedom*, an instrument called the *Ultra-High Resolution Spectroheliograph (UHRXS)*^{14,15}. The descoping of the *Freedom* caused the removal of all "attached payloads", including *UHRXS*¹⁶. We have discussed, elsewhere, several concepts which would permit the extension of the technology pioneered by *MSSTA* to achieve the capabilities discussed in iv, v, and vi on a free flying platform of modest size¹⁷⁻¹⁹, consistent with NASA's new philosophy of supporting small, focused missions which adhere tightly to pre-established schedules and budgets. We have also proposed the development of a polarimeter for the direct measurement of coronal magnetic fields²⁰⁻²³ (objective iv-c).

2.0 RECONFIGURATION OF THE *MSSTA*

The *MSSTA I* configuration has been described in detail previously²⁴⁻²⁶. The configuration of the *MSSTA I* as flown in May 1991 included seven Ritchey Chrétien telescopes of 127 mm aperture, which imaged narrow wavelength bands dominated by lines of H I, He II, C IV, O VI, Fe IX/X, Fe XII, and Fe XVI, a 75 mm aperture Herschel telescope also set to reflect Fe XII radiation, two 62.5 mm aperture Cassegrain telescopes which reflected Fe IX/X and Fe XIV radiation respectively, and four 38 mm aperture Herschel telescopes which reflected bands dominated by Ne V, Si XII, and Fe XX emission.

The details of the *MSSTA I* fabrication and launch are well documented. We briefly comment on the fabrication of several subsystems which have proven to be critical to the *MSSTA*'s successful performance. The *MSSTA* telescope mirror blanks were polished by Phil Baker of Baker Consulting, and the multilayer coatings were manufactured by T.W. Barbee, Jr. The rms surface finish of the Zerodur mirror blanks is ~ 2 Å. The central bandpasses of the multilayer coatings are all within ~ 0.5 % of the desired wavelength, and the reflectivities are typically ~ 70 % of the theoretical reflectivity for a perfect multilayer. Extensive optical tests with a He/Ne laser operating at 6328 Å have shown that the mirror figures are accurate to $\lambda/100$ at this wavelength, and should be diffraction limited at their operating wavelengths²⁷. The ultrasmooth mirror substrates are not expected to introduce significant scattering, even at resolving powers of 0.1 arc seconds. The *MSSTA* filters were fabricated by Luxel Inc. (Forbes Powell, President), and have met or exceeded their expected performance²⁸. The XUV 100 and 649 photographic emulsions used to record the *MSSTA* observations were manufactured by Kodak²⁹.

The power of the *MSSTA* for the study of the solar atmosphere is based on the sensitivity of the images recorded to the temperature of the solar structures observed, on the very high angular resolution of the images, and on the breadth of thermal coverage. The response of the *MSSTA* telescopes to the solar spectrum is given by the convolution of the telescope efficiency²⁷, $\epsilon(\lambda) = \epsilon_p \epsilon_s t_f$ [ϵ_p and ϵ_s represent the mirror reflectivities, and t_f the filter transmission], the solar emissivity, $E(\lambda, T)$ ²⁸⁻³⁰, and the response of the photographic film, $R(\lambda)$ ³¹⁻³³. The diagnostic power of the *MSSTA* telescopes is described by the function $K_n(T_e)$,

$$K_n(T) = \sum_{\lambda} z_{ij} \epsilon(\lambda) E(\lambda, T) \quad (1)$$

the sum extends over all radiative transitions (i-j) (including all population processes for the upper level i, and branching ratios to the lower level j) of all ionization stages, z, of all elements, Z. The reflectivities³⁴⁻³⁷, and filter transmissions^{37,38} of the *MSSTA I* telescopes have been described previously. The kernels, K_n , of the *MSSTA I* telescopes are described by DeForest *et al*³⁹; several response functions are shown in figure 3. Reviews of the performance of the *MSSTA* telescopes and the determination of absolute fluxes are presented by Allen *et al*^{40,41}.

The optical performance of the *MSSTA I* telescopes has been shown to approach 0.1 arc seconds on axis⁴²; the resolution of the solar images, therefore, depends on factors such as rocket jitter, and film resolution. The factors affecting the resolution of the *MSSTA I* telescopes have been discussed by Walker *et al*⁴³. The best images obtained by *MSSTA I* have ~ 0.7 arc seconds resolution³. Figure 4 shows the *MSSTA I* payload during prelaunch calibration at Marshall Space Flight Center and pre-launch activities at the White Sands Missile Range.

The principal changes incorporated for the *MSSTA II* launch are illustrated in figure 5, and are summarized below:

- (i). The *MSSTA* truss structure was modified to permit either a *f*/27 127 mm aperture Ritchey-Chretien, or a fast (*f*/8) 127 mm aperture Herschelian to be placed in positions VI and VII.
- (ii). The four 38mm aperture Herschelian telescopes placed in position B were replaced by a single 100 mm aperture *f*/18 Herschelian.
- (iii). Eight 38 mm aperture *f*/25 Herschelian telescopes were placed at positions α - θ .
- (iv). A bulkhead able to hold as many as five Pentax 645 cameras was added to record the images from the 127 mm and 38 mm Herschelians.

The actual *MSSTA II* flight configuration included six 127 mm Ritchey-Chretians, one 127 mm Herschelian, two 100 mm Herschelians, two 63 mm Cassegrains, and eight 38 mm Herschelians. The bandpasses and characteristics of the *MSSTA II* telescopes are in bold face type in Table 2. These modifications permit the *MSSTA* to record 17 images simultaneously, in as many as 17 bandpasses. The *MSSTA II* images were recorded on 14 cameras. Since some cameras can record more than one image, the *MSSTA II* images were recorded on 14 cameras.

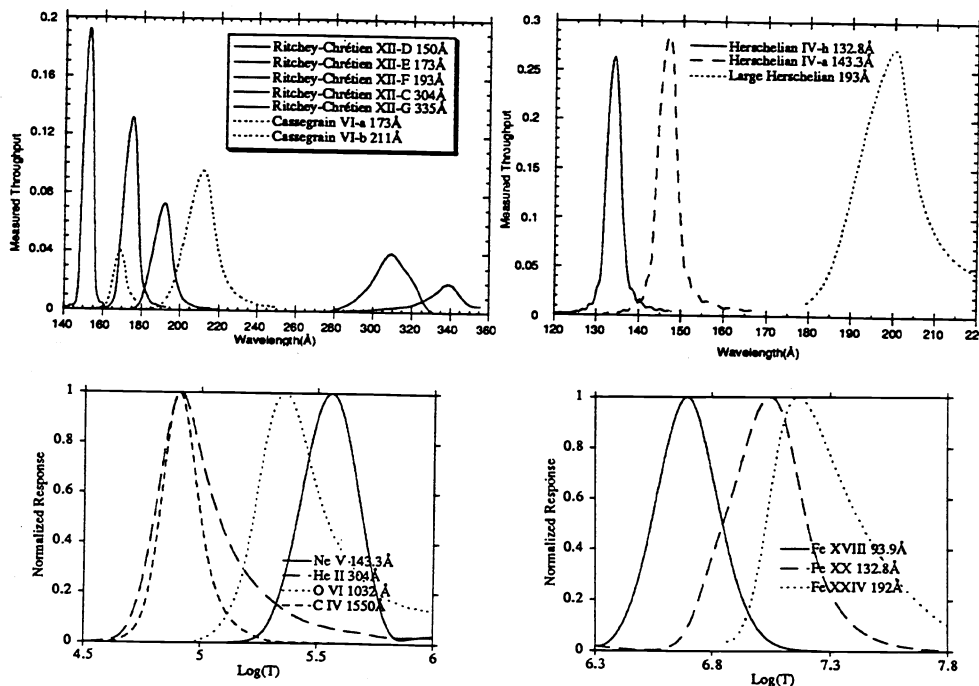


Figure 4. Efficiency, $\varepsilon(\lambda)$ (top panel), and thermal response $K_n(T_e)$ (lower panel) for several *MSSTA* telescopes.

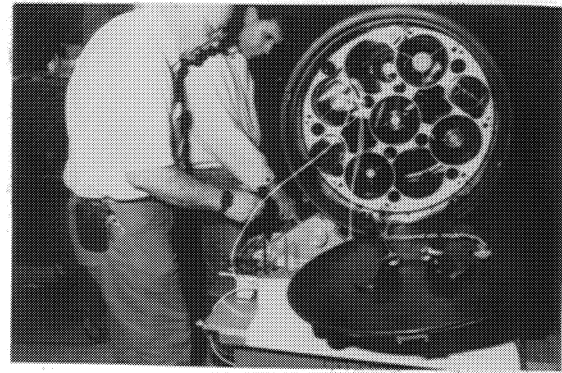
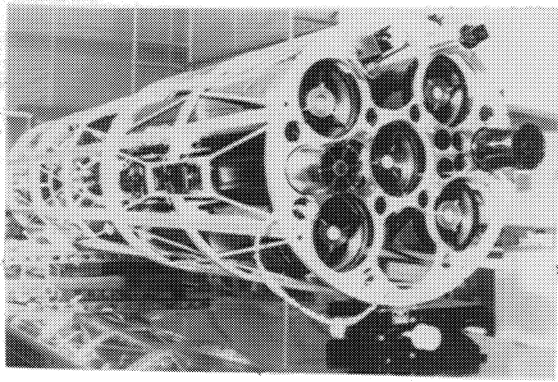


Figure 4. The *MSSTA* payload shown during prelaunch calibration at Marshall Space Flight Center.

The *MSSTA* payload being prepared for launch at White Sands Missile Range.

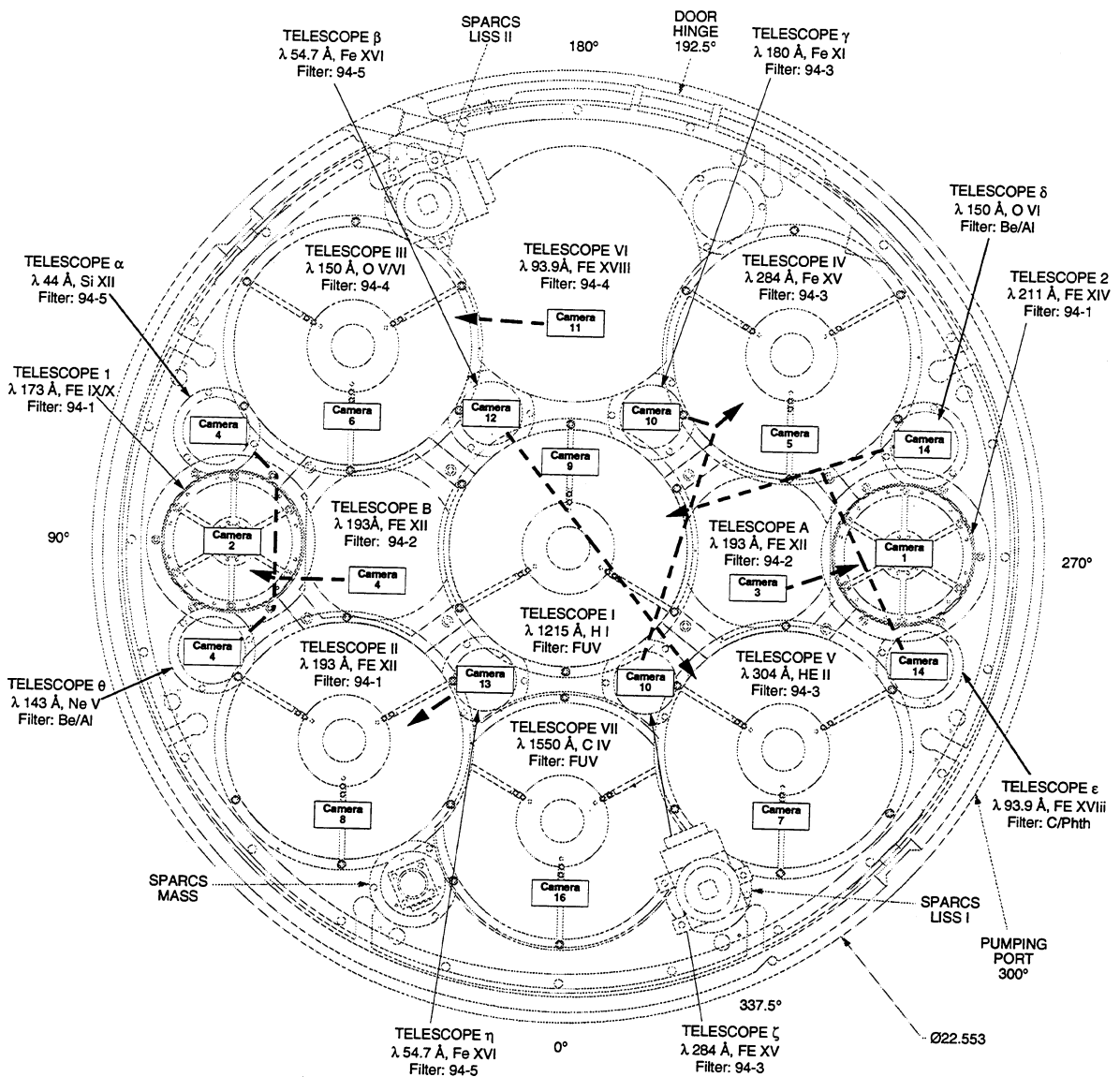


Figure 5. Front view of the *MSSTA* Rocket Observatory.

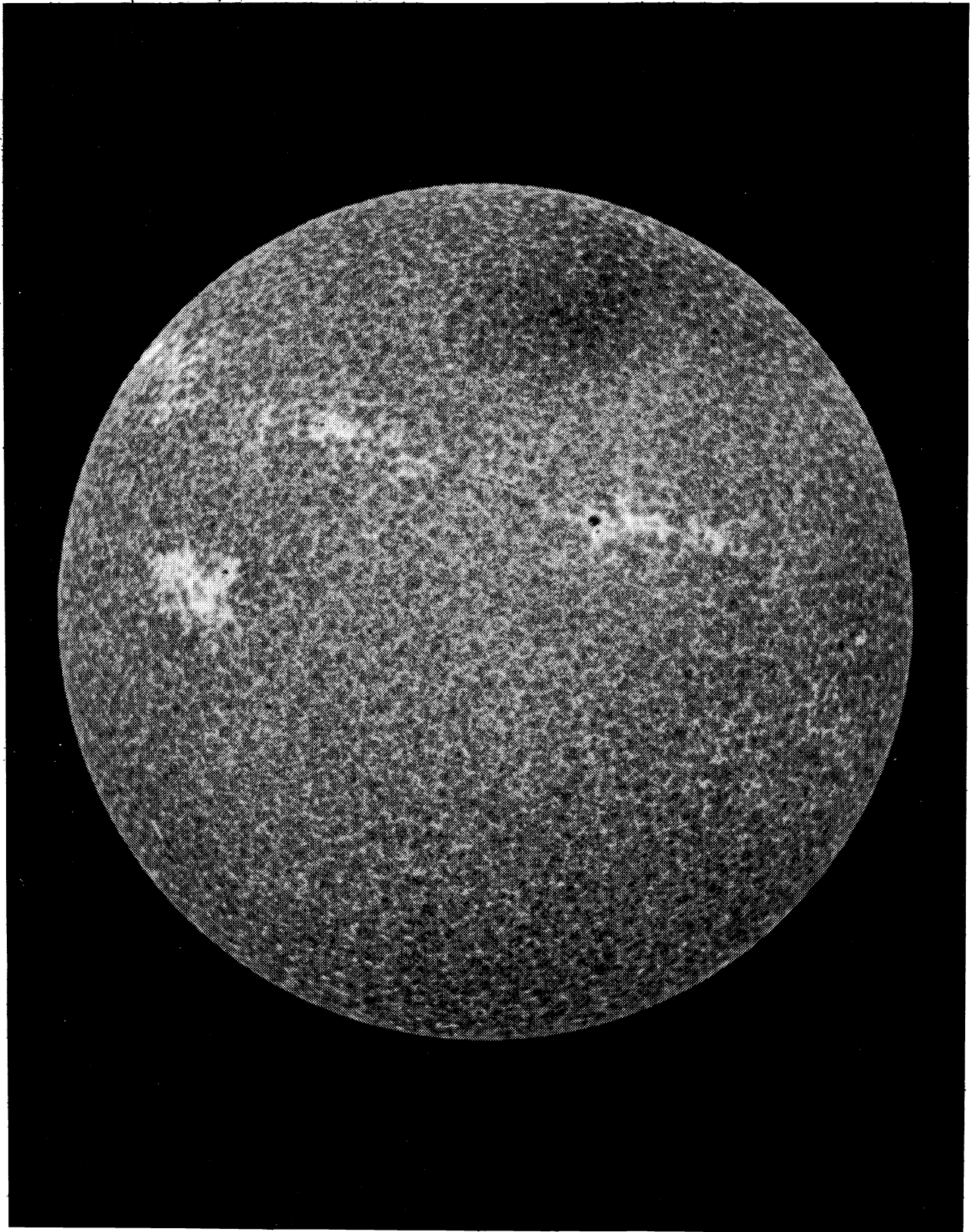


Figure 6. The chromosphere in the emission of Carbon IV at 1550 Å

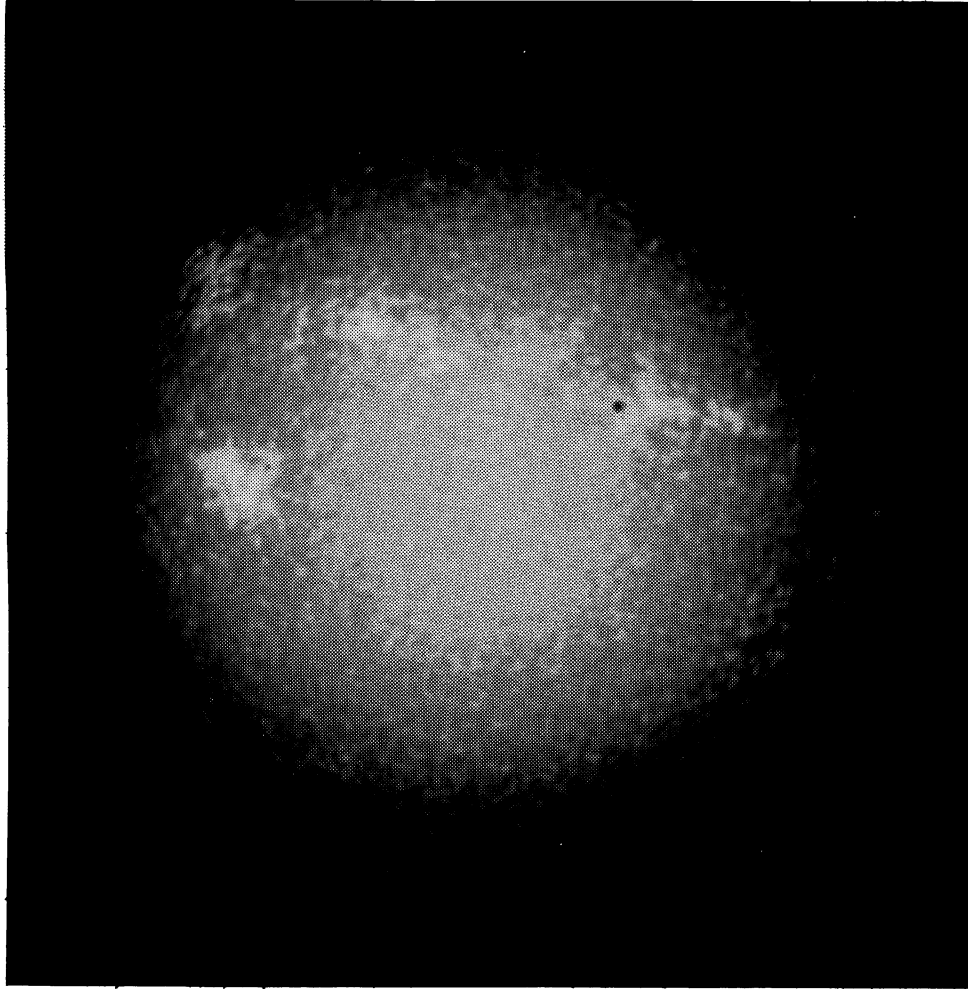


Figure 7a. H Ly α image of the chromospheric network, showing network structures.

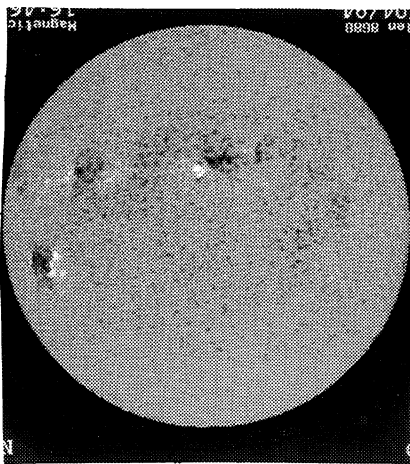


Figure 7b. KPNO Magnetogram.

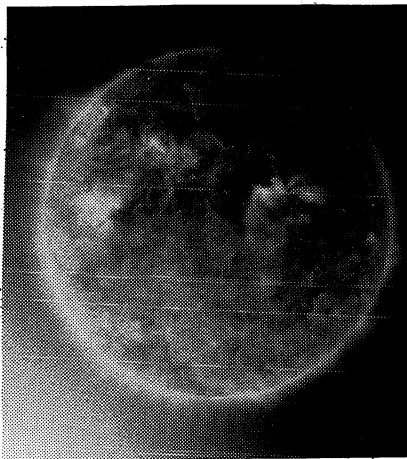


Figure 7c. Fe IX/X λ 173 Å image.

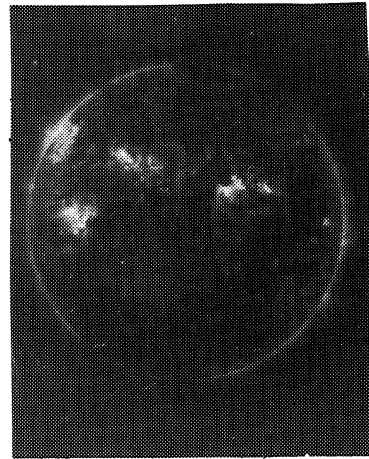


Figure 7d. Fe XI λ 180 Å image.

3.0 THE MSSTA II IMAGES

The *MSSTA II* was launched on November 3, 1994, at White Sands Missile Range. Because the launch occurred near the winter solstice, the look angles to the sun were rather unfavorable; coupled with a somewhat disappointing apogee, this resulted in significant absorption by the earth's atmosphere for wavelengths from $\sim 200 \text{ \AA} - 1000 \text{ \AA}$, causing many of our images to be quite faint. We expect to be able to enhance these images using digitized copies, and image processing techniques. Figures 6 and 7 represent 4 of the *MSSTA* images for which atmospheric absorption was not a serious problem. Figure 6, the chromosphere in C IV, provides a very high resolution view of the chromospheric network, and the network elements. We believe that the resolution exceeds 0.5 arc seconds, which is close to the diffraction limit of this telescope. The chromospheric network is also highly visible in the H Lyman α image in fig. 7a. Figure 7b shows chromospheric magnetic structure. Figures 7c and 7d show the corona at 173 \AA (Fe IX, O V, O VI, and Fe IX), and 180 \AA (Fe XI). The contrast between these two images is especially interesting, because the image centered at 173 \AA has contributions for lines of O V and O VI, which contribute $\sim 5\%$ of the total flux. These lines are excited in the temperature range 200,000 K to 350,000 K. The remainder of the flux in this bandpass is provided by the Fe IX and Fe X resonance lines, which are excited in the range 800,000 K to 1,300,000 K. The Fe IX $\lambda 180\text{\AA}$ image is dominated by lines excited at $\sim 1,100,000 \text{ K}$ to $1,500,000 \text{ K}$. This contrast between these images presents compelling evidence that the extended emission which is seen covering virtually the entire corona in figure 7b, is due to material which is below coronal temperatures, and may represent cool loops or funnels with temperatures in the range 200,000K to 300,000K.

MSSTA I images showed that some especially bright elements of the chromospheric network correspond to the footpoints of small loops or "coronal bright points". Conductive heating from the bright points appears to dominate the heating of these bright network elements. However, there were no coronal (*i.e.* with $T \sim 1,000,000 \text{ K}$ to $1,500,000 \text{ K}$) structures which could contribute to the heating of the majority of the chromospheric network elements. Figures 6 and 7 may provide evidence that the heating of most elements of the chromospheric network may have a significant contribution due to conduction from a new class of structures at temperatures in the range 200,000 K to 400,000 K. This possible link of the heating of chromospheric network elements by transition region structures at temperatures above 100,000 K is further strengthened by the fact that the network is significantly darker in the southern hemisphere (top of figure 6), where a large coronal hole and weak O V and O VI emission is indicated by figure 7c.

The resolution of the *MSSTA II* images appears to equal or exceed that of the *MSSTA I* images, especially the C IV image, which we believe approaches 0.5 arc seconds, close to the diffraction limit for this telescope.

References

1. R.G. Athay, "Radiation output," in *Physics of the Sun, Vol II*, P.A. Sturrock, T.E. Holzer, D.M. Mimihalas, R.K. Ulrich, eds., D. Reidel; Dordrecht, The Netherlands, 51, 1985.
2. E.M. Reeves, "The EUV chromospheric network in the quiet sun," *Solar Phys.* **46**, 53, 1976.
3. A.B.C. Walker, Jr., R.B. Hoover, and T.W. Barbee, Jr., "High Resolution Thermally Differentiated Images of the Chromosphere and Corona," to be published in *Advances in Stellar and Solar Coronal Physics: Proc. of the Vaiana Memorium Symposium*, J. Linsky, Ed., Kluwer Acad. Publ. Dordrecht 1992.
4. T. Berger, C.J. Schrijver, R.A. Shene, T.D. Tarbell, A.M. Title, and G. Scharmer, "New Observations of Sub-Arcsecond Photospheric Bright Points," submitted *Astrophys J.*, 1995.
5. R.J. Bray, L.E. Crain, C.J. Durrant and R.E. Roughhead, "*Plasma Loops in the Solar Corona*" Cambridge University Press, 1991.
6. T.W. Barbee, Jr., "Advances in multilayer x-ray/EUV optics: Synthesis, performance and instrumentation," *Optical Eng.* **29**, 711, 1990.
7. A.B.C. Walker, Jr., J.F. Lindblom, R.H. O'Neal, R.B. Hoover, and T.W. Barbee, Jr., "Astronomical observations with normal incidence multilayer optics: Present results and future prospects," *Phys. Scripta* **41**, 1053, 1990.
8. A.B.C. Walker, Jr. T.W. Barbee, Jr., R.B. Hoover, "Astronomical Observations with Normal Incidence Multilayer Optics II: Images of the Solar Corona and Chromosphere," *UV and X-Ray Spectroscopy of Astrophysical and Laboratory Plasmas: Proc. of the Tenth IAU International Colloquium*, Berkeley, CA. 1992, E.H. Silver and S.M. Kahn Eds. Cambridge Univ. Press, Cambridge, 193, 1993.
9. A.B.C. Walker, Jr., L. Jackson, J. Plummer, T.W. Barbee, Jr. and R.B. Hoover, "Astronomical Observations with Normal Incidence Multilayer Optics III: Selection of Multilayer Bandpass," *Proc. SPIE* **2011**, 1993.

10. A.B.C. Walker, Jr., J.E. Plummer, R. B. Hoover, T.W. Barbee, Jr., "Astronomical Observations with Normal Incidence Multilayer Optics IV: Selection of Spectral Lines," *Proc SPIE*, **2279**, 1994.
11. A.B.C. Walker, Jr., T.W. Barbee, Jr., R.B. Hoover, and J.F. Lindblom, "Soft x-ray images of the solar corona with a normal incidence multilayer Cassegrain telescope," *Science* **241**, 1781, 1988.
12. M. Zukic, D.G. Torr, J.F. Sparrn, and M.R. Torr, "Vacuum Ultraviolet Thin Films. 1: Optical constants of BaF₂, CaF₂, LaF₂, MgF₂, Al₂O₃, HfO₂ and SiO₂ thin films," *Appl. Optics* **29**, 4284 - 4292, 1990; M. Zukic, D.G. Torr, J.F. Spann and M.R. Torr, "Vacuum Ultraviolet Thin Films. 2: Vacuum Ultraviolet Dielectric Narrowband Filters," *Applied Opt.* **29**, 4293, 1990.
13. A.B.C. Walker, Jr., R.B. Hoover, and T.W. Barbee, Jr., "Chromospheric and coronal observations with multilayer optics," *Proc SPIE* **1742**, 515, 1992.
14. A.B.C. Walker, Jr., R.B. Hoover and T.W. Barbee, Jr., "Multi-Spectral Solar Telescope Array: Initial Results and Future Plans" *Proc SPIE*, **1742**, 500, 1992.
15. A.B.C. Walker, Jr., J.F. Lindblom, J.G. Timothy, M.J. Allen, C.E. DeForest, C. Kankelborg, R.H. O'Neal, E.S. Paris, and T.D. Willis, "The ultra high resolution XUV spectroheliograph, II: Predicted performance," *Proc. SPIE* **1343**, 319, 1990.
16. W.J. Broad, "NASA Reduces Cost and Role of Its Orbiting Space Station", *The New York Times*, March 5, 1991, p. 1.
17. A.B.C. Walker, Jr., J.F. Lindblom, J.G. Timothy, J.W. Barbee, Jr., R.B. Hoover, E. Tandbergen-Hanssen, S.T. Wu, J. Sahade, "The Solar/Stellar Coronal Explorer and the Solar/Stellar Coronal Observatory" , *Proc. SPIE*, **1546**, 281, 1991.
18. A.B.C. Walker, Jr., J.F. Lindblom, J.G. Timothy, R.B. Hoover, E. Tandberg-Hanssen, T.W. Barbee, Jr. "The Ultra High Resolution XUV Spectroheliograph III: A Modified Configuration for a Free Flying Platform" , *Proc. SPIE*, **1546**, 265, 1991.
19. A.B.C. Walker, Jr., J.G. Timothy, T.W. Barbee, Jr., and R B. Hoover , "Active Sun Telescope Array", *Proc. SPIE* **1343**, 334, 1990. .
20. S. Fineschi, R.B. Hoover, S. Fontenla, and A.B.C. Walker, Jr., "Solar EUV line polarimetry I: Observational parameters and theoretical considerations," *Proc. SPIE* **1343**, 316, 1990.
21. S. Fineschi, R.B. Hoover, and A.B.C. Walker, Jr., "Hydrogen Lyman α coronagraph polarimeter," *Proc. SPIE* **1546**, 412, 1991; "Polarimetry of H I Lyman α for coronal magnetic field diagnostics," these proceedings.
22. R.B. Hoover, S. Fineschi, A.B.C. Walker, Jr., R.B. Johnson, and M. Zukic, "Optical configurations of H I Lyman α coronagraph/polarimeters," *Proc. SPIE* **1546**, 414, 1991;
23. "Design and fabrication of the all-reflecting H Lyman α coronagraph/polarimeter," *Proc. SPIE* **1742**, 439, 1992.
24. A.B.C. Walker, Jr., J.F. Lindblom, R.H. O'Neal, M.J. Allen, T.W. Barbee, Jr., and R.B. Hoover, "The Multi-Spectral Solar Telescope Array," *Optical Eng* **29**, 581, 1990.
25. A.B.C. Walker, Jr., J.F. Lindblom, R.H. O'Neal, M.J. Allen, T.W. Barbee, Jr., R.B. Hoover, "The Multi-Spectral Solar Telescope Array", *Optical Eng* **29**, 581, 1990.
26. A.B.C. Walker, Jr., T.W. Barbee, Jr., R.B. Hoover, J.F. Lindblom, R.H. O'Neal, and P.C. Baker, "Performance of compact multilayer coated telescopes at soft x-ray, EUV and VUV wavelengths," *Optical Eng* **29**, 1281, 1990.
27. A.B.C. Walker, Jr., R.B. Hoover, and T.W. Barbee, Jr., "The Multi Spectral Solar Telescope Array VII: A Status Report," *Proc SPIE* **2011**, 1993.
28. J.F. Lindblom, R.H. O'Neal, A.B.C. Walker, Jr., F.R. Powell, T.W. Barbee, Jr., R.B. Hoover, and S.F. Powell, "The Multi-Spectral Solar Telescope Array IV: The soft x-ray and EUV filters," *Optical Eng.* **30**, 1134, 1991.
29. R Stern, E. Wang., and S. Bowyer, "Extreme ultraviolet spectrum of a hot interstellar plasma," *Astrophys. J. Suppl. Ser.* **37**, 195-222, 1978.
30. M. Landini, and B. C. Monsignori Fossi, "The X-UV spectrum of thin plasmas" *Astron. Astrophys. Suppl. Ser.* **82**, 229, 1990.
31. R.B. Hoover, A.B.C. Walker, Jr., C.E. DeForest, M.J. Allen, J.F. Lindblom, R.H. O'Neal, E.S. Paris, and A. DeWan, "The Multi-Spectral Solar Telescope Array VI: Performance and analysis of photographic film," *Proc. SPIE* **1343**, 175, 1990.
32. R.B. Hoover, A.B.C. Walker, Jr., C.E. DeForest, R.N. Watts, and C. Tarrío, "Ultra high-resolution photographic films for x-ray/EUV/FUV astronomy," *Proc SPIE* **1742**, 549, 1992.
33. R.B. Hoover, A.B.C. Walker, Jr., C.E. DeForest, M. Allen and D.B. Gore, "X-Ray/EUV/FUV Calibration of Photographic Films for Solar Research," *Proc SPIE* **2011**, 1993.

34. T.W. Barbee, Jr., J.W. Weed, Jr., R.B. Hoover, M. J. Allen, J.F. Lindblom, R.H. O'Neal, C.C. Kankelborg, C.E. DeForest, E.S. Paris, A.B.C. Walker, Jr., T.D. Willis, E. Gluskin, P. Pianetta, and P.C. Baker, "The Multi-Spectral Solar Telescope Array II: Reflectivity of the multilayer mirrors," *Optical Eng.* **30**, 1067, 1991.
35. M.J. Allen, *et al.*, "Calibration of the Multi-Spectral Solar Telescope Array Multilayer Mirrors and Filters", *Proc SPIE* **1742**, 562, 1992.
36. M.J. Allen, T.D. Willis, D. Martinez, C. Kankelborg, C.E. DeForest, R.H. O'Neal, A.B.C. Walker, Jr., T.W. Barbee, Jr., and R.B. Hoover, "Performance of compact multilayer coated telescopes II," *Proc SPIE* **2011**, 1993.
37. C.C. Kankelborg, J.E. Plummer, D.S. Martínez-Galarce, R.H. O'Neal, C.E. DeForest, A.B.C. Walker, Jr., R.B. Hoover, T. W. Barbee, "Calibration of multilayer mirrors for the Multi-Spectral Solar Telescope Array,"
38. J.F. Lindblom, R.H. O'Neal, A.B.C. Walker, Jr., F.R. Powell, T.W. Barbee, Jr., R.B. Hoover, and S.F. Powell, "The Multi-Spectral Solar Telescope Array IV: The soft x-ray and EUV filters," *Optical Eng.* **30**, 1134, 1991.
39. C.E. DeForest, C.C. Kankelborg, M.J. Allen, E.S. Paris, T.D. Willis, J.F. Lindblom, R.H. O'Neal, A.B.C. Walker, Jr., T.W. Barbee, Jr., R.B. Hoover, and T.W. Barbee, Jr., "The Multi-Spectral Solar Telescope Array V: Temperature diagnostic response to the optically thin solar plasma," *Optical Eng* **30**, 1125, 1991.
40. M.J. Allen, *et al.*, "Calibration of the Multi-Spectral Solar Telescope Array Multilayer Mirrors and Filters", *Proc SPIE* **1742**, 562, 1992.
41. M.J. Allen, T.D. Willis, D. Martinez, C. Kankelborg, C.E. DeForest, R.H. O'Neal, A.B.C. Walker, Jr., T.W. Barbee, Jr., and R.B. Hoover, "Performance of compact multilayer coated telescopes II," *Proc SPIE* **2011**, 1993.
42. R.B Hoover, *et al.*, "The Multi-Spectral Solar Telescope Array III: Optical characteristics of the Ritchey-Chrétien Telescopes," *Proc. SPIE* **1343**, 189, 1990.
43. A.B.C. Walker, Jr., J.F. Lindblom, J.G. Timothy, R.B. Hoover, T.W. Barbee, Jr., P.C. Baker, and F.R. Powell, "High resolution imaging with multilayer soft x-ray, EUV and FUV telescopes of modest aperture and cost," *Proc. SPIE* **1494**, 320, 1991.